PERGAMON

International Journal of Heat and Mass Transfer 43 (2000) 1651–1659

International Journal of HEAT and MASS TRANSFER

www.elsevier.com/locate/ijhmt

Heat transfer and friction characteristics of fin-and-tube heat exchangers

Wei-Mon Yan*, Pay-Jen Sheen

Department of Mechanical Engineering, Huafan University, Shih Ting, Taipei 22305, Taiwan, ROC

Received 26 February 1999

Abstract

An experimental study has been carried out to investigate the heat transfer and pressure drop characteristics of fin-and-tube exchangers with plate, wavy and louvered fin surfaces. In all, 36 samples of heat exchangers, including 12 plate-fin, 12 wavy-fin and 12 louvered-fin geometries, were tested. Results are presented as plots of friction factor f and Colburn j factor against Reynolds number in the range 300–2000. Additionally, the dimensional heat transfer coefficient and pressure drop are also presented against frontal air velocity. Finally, various comparison methods were adopted to evaluate the air side performance of the plate, wavy and louver fin heat exchangers.

1. Introduction

Heat exchangers with fins and round tubes are widely used in industrial, air-conditioning and refrigeration applications to meet the demand for saving energy and resources. To reduce size and weight of heat exchangers, various fin patterns have been developed to improve the air-side heat transfer performance. Typical fin geometries are plate, wavy and louver fin surfaces. Generally, the complexity of the air flow pattern across the fin-and-tube exchangers makes the numerical simulation very difficult. Accordingly, it is necessary to resort to experimental study.

Recently, Kayansayan [1] investigated the effects of outer surface geometry on the performance of flat plain fins and round tube heat exchangers with four-row coils. A combined numerical and experimental study of plate-fin and tube heat exchangers was examined by Jang et al. [2]. In their study, the detailed numerical results of pressure drop and heat transfer coefficient are presented, but experimental results are little. A systematic study on heat and friction characteristics of plate fin-and-tube heat exchangers was experimentally investigated by Wang et al. [3]; the results are limited to the cases with large fin pitch heat exchangers. Beecher and Fagan [4] reported heat transfer data for twenty wavy geometries. Similar studies were also examined experimentally by Mirth and Ramadhyani [5], Wang et al. [6] and Youn et al. [7].

As the performance of the fin-and-tube heat exchangers depends on the pattern of fins, the louver surface can break and renew the boundary layer of the air flow, and consequently, higher heat transfer performance would be expected as compared with plain fins. Kays and London [8] were the first to report heat transfer and pressure drop data on louvered fins. Achaichia and Cowell experimentally studied [9] and numerically examined [10] the heat transfer and pressure drop characteristics of flat tube and louvered fin surfaces. To understand the detailed flow pattern

* Corresponding author. Fax: +886-2-26633847.
E-mail address: wmyan@huafan.hfu.edu.tw (W.-M. Yan).

0017-9310/00/$ - see front matter
PII: S0017-9310(99)00229-X

Nomenclature

A	area [m^2]
A_o	total surface area [m^2]
A_t	external tube surface area [m^2]
c_p	specific heat at constant pressure [J/(kg K)]
C	heat capacity rate [W/K]
D_c	fin collar outside diameter [m]
D_h	hydraulic diameter [m]
D_i	inside tube diameter [m]
D_o	outside tube diameter [m]
f	Fanning friction factor
F	fin pitch [m]
G_c	mass flux of the air based on the minimum flow rate [kg/(m^2 s)]
h	heat transfer coefficient [W/(m^2 K)]
j	Colburn j factor, $Nu/(Re_{D_c}Pr^{1/3})$
k	thermal conductivity [W/(m K)]
K_c	abrupt contraction pressure-loss coefficient
K_e	abrupt expansion pressure-loss coefficient
$\dot{m}$	mass flow rate [kg/s]
N	number of longitudinal tube rows
Nu	Nusselt number, hD_c/k
NTU	number of transfer units
Pr	Prandtl number, ν/α
P_t	transverse tube pitch [m]
P_l	longitudinal tube pitch [m]
$\dot{Q}$	heat transfer rate [W]
Re_{D_c}	Reynolds number, $\rho V D_c/\mu$
S_2	heat transfer power per unit temperature difference and per unit core volume, Eq. (11)
S_3	friction power expenditure per unit core volume, Eq. (12)
t	fin thickness [m]
T	temperature [°C]
U	overall heat transfer coefficient [W/(m^2 K)]
V	velocity [m/s].

Greek symbols

δ	wall thickness [m]
ΔP	pressure drop [Pa]
ϵ	heat transfer effectiveness, $\dot{Q}_{ave}/\dot{Q}_{max}$
η	fin efficiency
η_o	surface effectiveness
μ	dynamic viscosity of air [Pa s]
ρ	density of air [kg/m^3]
σ	contraction ratio of cross-sectional area.

Subscripts

1	air-side inlet
2	air-side outlet
air	air side
ave	average value
f	fin pitch
i	tube side
in	inlet
min	minimum value
max	maximum value
o	total surface
out	outlet
water	water side
w	wall of tube.

across the fin-and-tube heat exchanger, Webb and Trauger [11] performed a flow visualization study of the louvered fin geometry with a flat tube. An analytical model for predicting air-side heat exchanger performance of louvered fin geometry was developed by Sahnoun and Webb [12]. Their model is based on boundary layer and channel flow equations, and accounts for the flow efficiency. All the studies reviewed here are limited to the results of louver fins with a flat tube. The louver fin-and-tube heat exchangers with round tube are more popular in the HVAC&R applications. Hence, experimental studies of heat transfer and friction characteristics of typical louver fin-and-tube heat exchangers were performed by Wang et al. [13,14], but the effects of fin spacing and number of tube rows on the heat transfer coefficient and pressure drop did not appear in their studies. Therefore, the extensive experimental results of the louver fin configuration are of importance in the HVAC&R applications.

Despite this, there are numerous experimental data related to the fin-and-tube heat exchangers; however, detailed performance comparisons among these fin patterns are still limited. Therefore, this motivates the present study to quantitatively compare the performance of various fin-and-tube heat exchangers.

2. Experimental apparatus

Thirty-six heat exchangers of various fin geometries and in staggered configuration with various tube row and fin pitch combinations were examined in this work. The detailed geometrical parameters are tabulated in Table 1. A wind tunnel facility similar to the

Table 1
The sizes of the fin-and-tube heat exchangers

No.	Staggered (s)	Fin pitch t (mm)	D_c (mm)	P_t (mm)	P_l (mm)	Row no.
1	S	1.4	10.3	25.4	19.05	1
2	S	1.4	10.3	25.4	19.05	2
3	S	1.4	10.3	25.4	19.05	3
4	S	1.4	10.3	25.4	19.05	4
5	S	1.69	10.3	25.4	19.05	1
6	S	1.69	10.3	25.4	19.05	2
7	S	1.69	10.3	25.4	19.05	3
8	S	1.69	10.3	25.4	19.05	4
9	S	2.0	10.3	25.4	19.05	1
10	S	2.0	10.3	25.4	19.05	2
11	S	2.0	10.3	25.4	19.05	3
12	S	2.0	10.3	25.4	19.05	4

one used in previous fin-and-tube heat exchanger experiments [3,13,14] was modified, as shown in Fig. 1, to conduct this study. A schematic diagram of the wind tunnel system is designed to suck room air over the finned side of the exchanger by a 3.73 kW centrifugal fan with an inverter while circulating hot water through the tubes. The tunnel was a rectangular duct 60 × 40 cm in cross section. To minimize heat

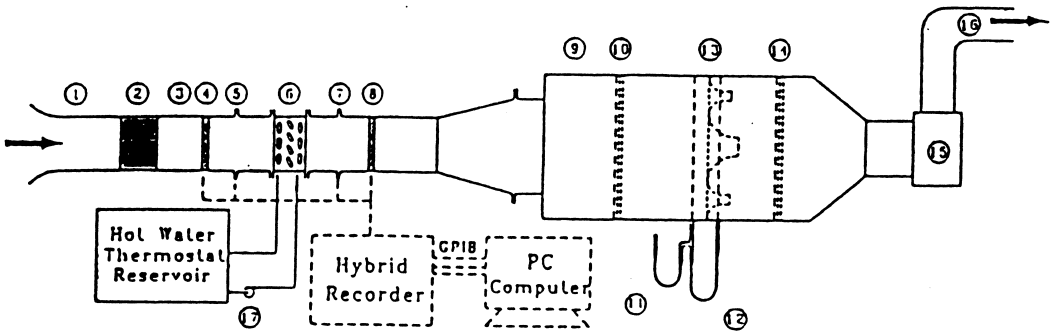

1 Inlet
2 Honey cone straightener
3 Developing section
4 Pressure tap (inlet)
5 Test unit
6 Pressure tap (outlet)
7 T/C outlet temperature measuring station
8 Setting means
9 Code tester for measurement of air flow rate
10 Setting means
11 Nozzle pressure tap (inlet)
12 Nozzle pressure tap (outlet)
13 Multiple nozzles plate
14 Setting means
15 Variable exhaust fan system
16 Discharge
17 Water pump

Fig. 1. Schematic of the test facility.

loss to the surroundings, the tunnel surface is insulated with a 2 cm thick glass wool layer. Being supported by stands of perforated steel plates, the tunnel system is evaluated 80 cm above the floor level of the laboratory.

The inlet and exit temperatures across the air side of the heat exchangers are measured by two T-type thermocouple meshes. The inlet measuring mesh consists of eight thermocouples while the exit mesh contains twelve thermocouples. These data signals are individually recorded and then averaged. The working medium on the tube side was hot water. The water circulation supplies high-velocity hot water to the tube side. The water is heated by a 80 kW electric heater, whose power input is adjustable. Both the inlet and outlet temperatures were measured by two pre-calibrated RTDs (Pt-100 Ω) which have an accuracy of 0.1°C. The water flow rate was measured by a calibrated magnetic flow meter with 0.002 l/s resolution. During the experiments, the water inlet temperature was kept constant at 60°C with volume flow rate 10 l/min.

The air pressure drops across the heat exchanger and the nozzles are, respectively, measured by precision differential pressure transducers, reading to 0.1 Pa. The air flow measuring station is a multiple nozzle code tester based on the ASHRAE 41.2 standard [15].

The heat exchanger, with specified surface geometry, was installed in the test system. In this work, the exchanger height was less than the tunnel dimensions, and the bypass flows were eliminated by a thin layer of foam plastic sandwiched between the edges of the fins and the casing. Upon completion of the hot water side links, the coil was completely insulated with a 3 cm thick layer of glass wool. The air flow through the test section was adjusted to a desired value by a converter. In addition, the inlet water was kept at 60°C with a fixed flow rate. If the test system including the air and water sides becomes steady state, the data signals were recorded.

3. Data correlation

3.1. Pressure drop

The core friction of the heat exchanger was reduced to obtain the Fanning friction factor f. In the present study, the pressure drop equation proposed by Kays and London [8], including the entrance and exit pressure losses, was used to evaluate the friction factor. The equation is

$$f=\left(\frac{A_c}{A_o}\right)\left(\frac{\rho_m}{\rho_1}\right)\left[\frac{2\rho_1\Delta P}{G_c^2}-(K_c+1-\sigma^2)-2\left(\frac{\rho_1}{\rho_2}-1\right)+(1-\sigma^2-K_e)\left(\frac{\rho_1}{\rho_2}\right)\right] \tag{1}$$

where A_c and A_o are the minimum flow area and total heat transfer area, respectively. K_c and K_e are the inlet and exit heat loss coefficients, respectively, and σ means the ratio of the minimum flow area to the frontal area. The entrance and exit loss coefficients, K_c and K_e, are adopted from Figs. 14–26 from McQuiston and Parker [16].

3.2. Heat transfer

In the study of heat exchanger performance, the Colburn j factor is of interest. To obtain the j factor from the experimental data, the effective-NTU equation with unmixed–unmixed cross flow is employed to determine the UA-value. The ϵ–NTU relation is [8,16]

$$\epsilon=1-\exp\frac{\mathrm{NTU}^{0.22}}{C^*[\exp(-C^*\mathrm{NTU}^{0.78}-1)]} \tag{2}$$

where

$$C^*=\frac{C_{\min}}{C_{\max}}=\frac{(\dot m c_p)_{air}}{(\dot m c_p)_{water}} \tag{3}$$

$$\epsilon=\frac{\dot Q_{ave}}{\dot Q_{max}}=\frac{\dot Q_{ave}}{(\dot m c_p)_{air}(T_{in,\,water}-T_{in,\,air})} \tag{4}$$

$$\mathrm{NTU}=\frac{UA}{C_{\min}} \tag{5}$$

The total heat transfer rate $\dot Q_{ave}$ is calculated as the average of the air- and water-side values. With Eqs. (2)–(5), an iterative procedure is needed to obtain the overall heat transfer coefficient UA. The air-side thermal resistance, $1/(\eta_o h_o A_o)$, was evaluated by subtracting the water-side and wall thermal resistances from the total thermal resistance, assuming zero water-side fouling resistance, where h_o is the air-side heat transfer coefficient and η_o is the surface effectiveness. η_o is defined as the actual heat transfer for the fin and base divided by the heat transfer for the fin and base when the fin is at the same base temperature. The detailed evaluation of η_o is available in Refs. [3,18]. For the study of performance of heat exchangers, the Colburn j factor is of interest. Thus,

$$\left(\frac{1}{\eta_o h_o A_o}\right)=\frac{1}{UA}-\frac{1}{h_i A_i}-\frac{\delta_w}{k_w A_w} \tag{6}$$

Note that the second term of the right-hand-side of Eq. (6) indicates the wall-side thermal resistance and the third term means the tube wall resistance. The tube-side heat transfer coefficient, h_i, was calculated by the Petukhov correction for turbulent flow in tubes [17]. That is,

$$h_i = \left(\frac{k}{D}\right)_i Re_i Pr \frac{(f_i/2)}{1.07 + 12.7(f_i/2)^{0.5}(Pr^{2/3} - 1)} \tag{7}$$

with the friction factor given by

$$f_i = 1/[1.58\ \ln(Re_i) - 3.28]^2 \tag{8}$$

The Colburn j factor is defined as

$$j = \frac{Nu}{Re_{D_c}\, Pr^{1/3}} \tag{9}$$

where the Nusselt number is

$$Nu = \frac{h_o D_c}{k_{air}} \tag{10}$$

The Reynolds number, Re_i, is up to about 20,000 in the present study.

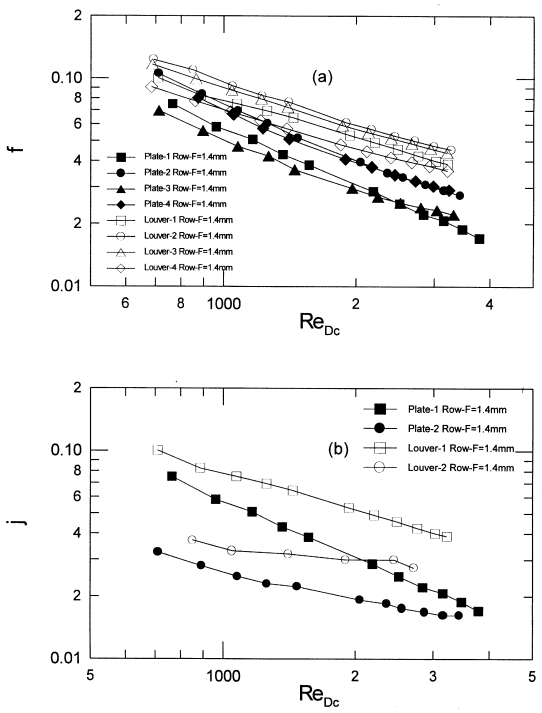

Fig. 2. Effects of tube row number on the f and j factors.

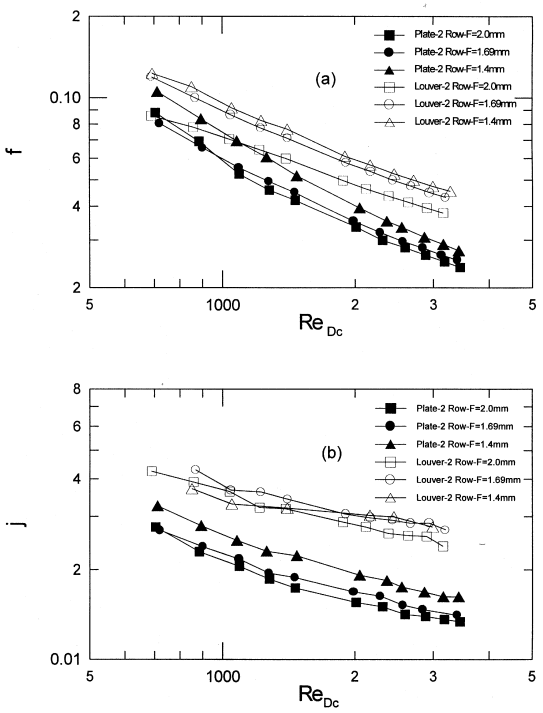

Fig. 3. Effects of fin pitch on the f and j factors.

4. Results and discussion

4.1. f and j factors vs Reynolds number

The basic surface characteristics of heat exchangers are generally presented in dimensionless form as the Fanning friction factor f and the Colburn j factor. Fig. 2 shows the effects of the tube row number on the f and j factors against the Reynolds number Re_{D_c}. The Reynolds number Re_{D_c} is based on the outer tube diameter (including collar thickness). Both f and j factors decrease with increasing Re_{D_c}. Comparison of the results between plate and louver fin heat exchangers shows that larger f and j factors are found for the louver fin heat exchangers.

Fig. 3 presents the effects of fin pitch on the f and j factors for various fin patterns with identical tube row numbers. The fin pitches are 2.0, 1.69 and 1.4 mm, respectively. For plate fin heat exchangers, the f and j factors increase with the decrease in the fin pitch. But for louver fin heat exchangers, the effects of fin pitch on the f and j factors do not show a trend.

4.2. ΔP and h vs frontal air velocity V

The results of pressure drop ΔP and heat transfer coefficient h are also important for the designers of

heat exchangers. As expected, both ΔP and h increase with the frontal air velocity, V. Better ΔP and h performances are found from Figs. 4 and 5 for louver fin heat exchangers. In Fig. 4(a), a larger ΔP will be found for a heat exchanger with a greater tube row number. But for heat transfer coefficient, h in Fig. 4(b), the effects of the tube row number on h shows an insignificant influence. Like the results of fin pitch on the friction factor f, ΔP decreases with the increase in the fin pitch.

4.3. Comparison of $\sigma^2 j/f$

Fig. 6 shows the comparison "area of goodness factor", $\sigma^2 j/f$, vs the Reynolds number Re_{D_c} for plate, wavy and louver fin exchangers. An overall inspection on Fig. 6 discloses that for tube row 1 heat exchanger, the wavy fin geometry shows the highest value of $\sigma^2 j/f$ under the same Re_{D_c}, and the plate fin comes in second while the louver fin shows the lowest. But for tube row 2 heat exchangers, the plate fin surface gives the lowest values of $\sigma^2 j/f$.

4.4. Volume goodness factor comparison

In this present study, another comparison of the heat exchanger performance is taken as the volume

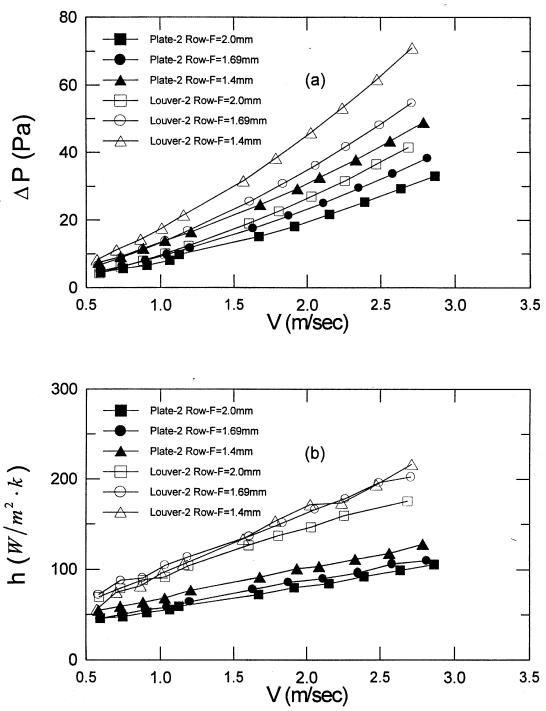

Fig. 5. Effects of fin pitch on ΔP and h.

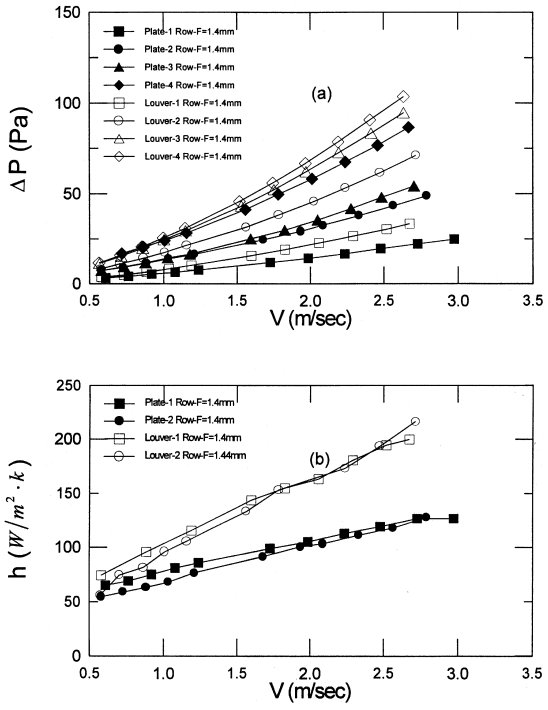

Fig. 4. Effects of tube row number on ΔP and h.

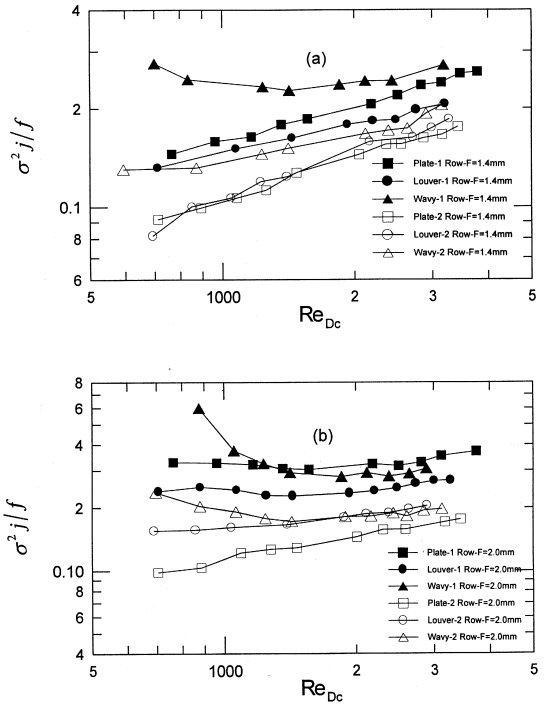

Fig. 6. Comparison of $\sigma^2 j/f$.

goodness factor comparison suggested below:

$$S_2 = \frac{c_p \mu \eta_o}{(Pr^{2/3})(4\sigma/D_h^2) j\, Re} \tag{11}$$

$$S_3 = \frac{\mu^3}{(2\rho^2)(4\sigma/D_h^4) f\, Re^3} \tag{12}$$

where S_2 means the heat transfer power per unit temperature difference and per unit core volume; S_3 indicates the friction power expenditure per unit core volume. From the viewpoint of heat exchanger volume required, a larger S_2 vs S_3 is better for a designer of heat exchanger. Fig. 7 presents the S_2 vs S_3 for plate, wavy and louver fin heat exchangers having $F = 1.4$ and 2.0 mm. It is clear that for a given S_3, a higher S_2 is found for a case with a lower tube row number. Additionally, a largest S_3 is found for a louver fin surface. This means that for a fixed volume of heat exchanger, the louver fin heat exchanger shows a better performance.

4.5. Heat transfer coefficient vs fan power

To evaluate overall performance of the heat exchanger, it would be necessary to consider heat transfer and pressure drop at the same time, and the concept of fan power per unit frontal area is introduced, which

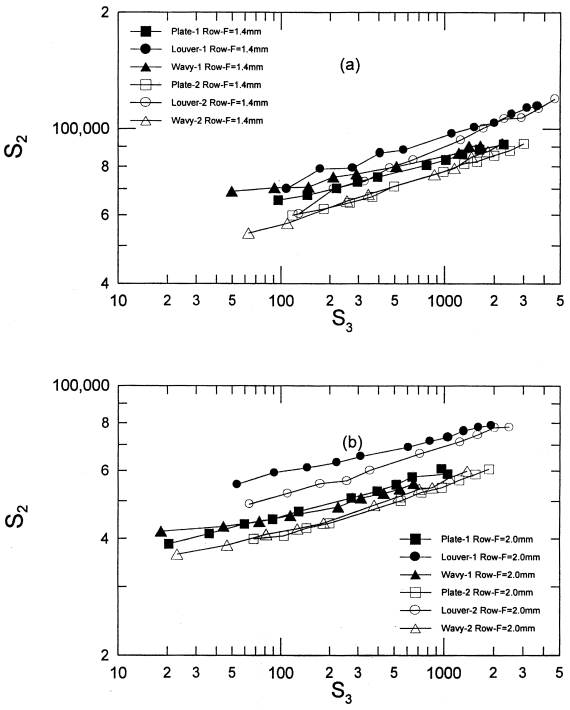

Fig. 7. Volume goodness comparison for tube rows 1 and 2.

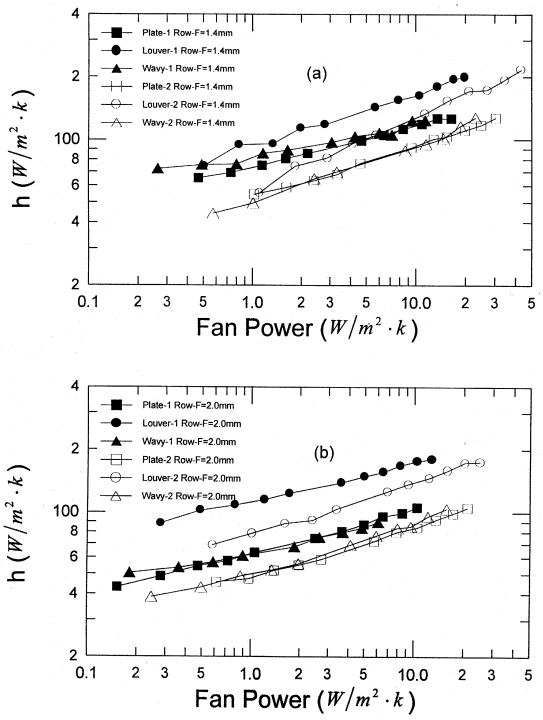

Fig. 8. Comparison of h vs fan power.

is defined as follows:

$$\text{Fan power per unit frontal area} = \text{frontal velocity } V \times \text{pressure drop } \Delta P = V\Delta P \tag{13}$$

In Fig. 8, the heat transfer coefficient of plate, wavy and louver fins of tube rows 1 and 2 are compared with respect to the fan power. An overall inspection of Fig. 8 reveals that at a fixed fan power, a better heat transfer coefficient h is found for a heat exchanger with a lower tube row number ($=1$). In addition, the louver fin surface shows the largest h among various fin surfaces. This means the louver fin is relatively most advantageous when used at the same operating condition.

4.6. Comparison using VG-1 criteria

A practical air-side performance may be made using the VG-1 criteria of Webb [19], which measures the possible reduction of the surface area. This methodology compares the required total air-side surface area (A) for fixed values of the fan power, heat duty, and temperature difference. Fig. 9 presents the ratio A/A_{plate} against Reynolds number Re_{D_c}. The ratio A/A_{plate} is defined as [19]:

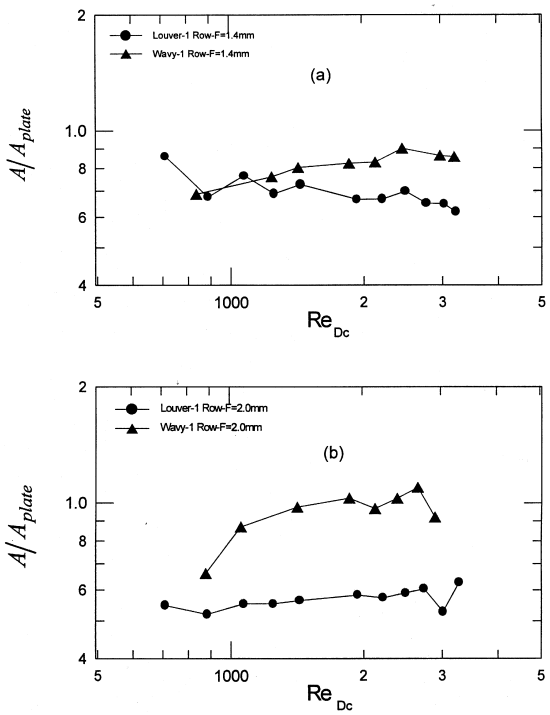

Fig. 9. Ratios of fin surfaces are relative to plate fin using VG-1 criteria.

$$\frac{A}{A_{\text{plate}}} = \left(\frac{f}{f_{\text{plate}}}\right)^{1/2}\left(\frac{j_{\text{plate}}}{j}\right)^{3/2} \tag{14}$$

where A_{plate} is the plate fin geometry. As expected, approximately 30% area reduction is seen for the louver fin surface having fin pitch $F = 1.4$ mm. For fin pitch $F = 2.0$ mm, the louver fins require approximately 40% less fin surface than the plate fin to yield the same heat transfer performance. This indicates that for the same Reynolds number Re_{D_c}, a larger area reduction is encountered for a system with a larger fin pitch.

5. Conclusions

An experimental study of the air-side heat transfer and pressure drop characteristics of plate, wavy and louver fin surfaces was carried out. Thirty-six samples of plate, wavy and louver fin-and-tube heat exchangers with different fin pitch and tub row number were tested. Various comparison methods have been adopted to evaluate the performance of the heat exchanger among various fin surfaces. The following conclusions are made:

1. at the same Re_{D_c}, a louver fin geometry shows larger values of f and j factors, compared with the plate fin surface;
2. at the same frontal velocity, the pressure drop ΔP increases with increasing tube row numbers;
3. the wavy fin heat exchanger has the highest $\sigma^2 j/f$ ratio for $Re_{D_c} \leqq 1500$ among the plate, wavy and louver heat exchangers;
4. for volume goodness factor comparison, louver fin heat exchangers have the highest S_2 at a given S_3;
5. for comparison using VG-1 criteria, about 40% surface area reduction was found for a louver fin heat exchanger, relative to the plate fin heat exchangers, and the area reduction increases with the fin pitch.

Acknowledgements

The support of this work by the National Science Council, ROC, under contract No. NSC 87-2212-E211-006 is gratefully acknowledged. Additionally, the valuable suggestions from Dr C. C. Wang are very much appreciated.

References

[1] N. Kayansayan, Heat transfer characterization of flat plain fins and round tube heat exchangers, Exper. Thermal Fluid Science 6 (1993) 263–272.
[2] J.Y. Jang, M.C. Wu, W.J. Chang, Numerical and experimental studies of three-dimensional plate-fin and tube heat exchangers, Int. J. Heat Mass Transfer 39 (1996) 3057–3066.
[3] C.C. Wang, Y.J. Chang, Y.C. Hsieh, Y.T. Lin, Sensible heat and friction characteristics of plate fin-and-tube heat exchangers having plate fins, Int. J. Refrigeration 19 (1996) 223–230.
[4] D.T. Beecher, T.J. Fagan, Effects of fin pattern on the air-side heat transfer coefficient in plate finned-tube heat exchangers, ASHRAE Trans. 93 (2) (1987) 1961–1984.
[5] D.R. Mirth, S. Ramadhyani, Corrections for predicting the air side Nusselt numbers and friction factors in child water cooling coils, Exp. Heat Transfer 7 (1994) 144–162.
[6] C.C. Wang, W.L. Fu, C.T. Chang, Heat transfer and friction characteristics of typical wavy fin-and-tube heat exchanger, Exper. Thermal Fluid Science 14 (1997) 174–186.
[7] B. Youn, Y.H. Kil, H.Y. Park, K.C. Yoo, Y.S. Kim Experimental study of pressure drop and heat transfer characteristics of ϕ10.07 wave and wave-slit fin-tube heat exchangers with wave depth of 2 mm. In: Proceedings of the 11th Heat Transfer Conference, Kyongju, Korea, 1998, 6, pp. 333–338.
[8] W.M. Kays, A.L. London, Compact Heat Exchangers, 3rd ed., McGraw-Hill, New York, 1984.

[9] A. Achaichia, T.A. Cowell, Heat transfer and pressure characteristics of flat tube and louvered plate fin surfaces, Exper. Thermal Fluid Science 1 (1988) 147–157.
[10] A. Achaichia, T.A. Cowell A finite difference analysis of fully developed periodic laminar flow in inclined louver arrays. In: Proceedings of the Second UK National Heat Transfer Conference, Glasgow, UK, 1988, 2, pp. 883–888.
[11] R.L. Webb, P. Trauger, Flow structure in the louvered fin heat exchanger geometry, Exper. Thermal Fluid Science 4 (1991) 205–217.
[12] A. Sahnoun, R.L. Webb, Prediction of heat transfer and friction for the louver fin geometry, ASME J. Heat Transfer 114 (1992) 893–900.
[13] C.C. Wang, P.Y. Chen, J.Y. Jang, Heat transfer and friction characteristics of convex-louver fin-and-tube exchangers, Exp. Heat Transfer 9 (1996) 61–78.
[14] C.C. Wang, K.Y. Chi, Y.J. Chang, An experimental study of heat transfer and friction characteristics of typical louver fin-and-tube heat exchangers, Int. J. Heat Mass Transfer 41 (1999) 817–822.
[15] ASHRAE Standard 41.2-1987 Standard Methods for Laboratory Air-flow Measurement, 1987.
[16] F.C. McQuiston, J.D. Parker, in: Heating, Ventilation, and Air-conditioning Analysis and Design, 4th ed., Wiley, New York, 1994, p. 571 (Chap. 14).
[17] B.S. Petukhov, V.A. Jurganov, A.I. Gladuntsov, Heat transfer in turbulent pipe flow of gases with variable properties, Heat Transfer, Sov. Res. 5 (1973) 109–116.
[18] Th.E. Schmidt, Heat transfer calculation for extended surfaces, Refrig. Eng. 49 (1949) 351–357.
[19] R.L. Webb, Principles of Enhanced Heat Transfer, Wiley, New York, 1994.